Published in final edited form as:
J Comp Neurol. 2006 December 1; 499(4): 645–661.

Innervation of Orexin/Hypocretin Neurons by GABAergic, Glutamatergic or Cholinergic Basal Forebrain Terminals Evidenced by Immunostaining for Presynaptic Vesicular Transporter and Postsynaptic Scaffolding Proteins

PABLO HENNY and **BARBARA E. JONES***
Montreal Neurologiclal Institute, McGill University, Montreal, Quebec H3A 2B4, Canada

Abstract

Orexin/hypocretin (Orx) neurons are critical for the maintenance of waking in association with behavioral arousal and postural muscle tone, since with their loss narcolepsy with cataplexy occurs. Given that basal forebrain (BF) neurons project to the hypothalamus and play important diverse roles in sleep/wake states, we sought to determine whether acetylcholine (ACh), glutamate (Glu), and/or GABA-releasing BF neurons innervate and could thereby differentially regulate the Orx neurons. From discrete injections of biotinylated dextran amine (BDA, 10,000 MW) into the magnocellular preoptic nucleus (MCPO) and substantia innominata (SI) in the rat, BDA-labeled fibers projected to the lateral hypothalamus (LH), perifornical area (PF), and dorsomedial hypothalamus (DMH), where ~41%, ~11%, and 9% of Orx-positive (+) neurons were respectively contacted in each region. Employing triple fluorescent staining for Orx, BDA, and presynaptic vesicular (V) transporters (T), we found that only 4% of the innervated Orx+ neurons in the LH were contacted by BDA+ [VAChT +] terminals, whereas ~31% and ~67% were respectively contacted by BDA+ [VGluT2+] and BDA + [VGAT+] terminals. In 3D-rendered and rotated confocal images, we confirmed the latter contacts and examined staining for postsynaptic proteins PSD-95, a marker for glutamatergic synapses, and gephyrin, a marker for GABAergic synapses, that were located on Orx+ neurons facing BDA-labeled terminals in ~20% and ~50% of contacts, respectively. With such synaptic input, BF glutamatergic neurons can excite Orx neurons and thus act to maintain behavioral arousal with muscle tone, whereas GABAergic neurons can inhibit Orx neurons and thus promote behavioral quiescence and sleep along with muscle atonia.

Indexing terms

BDA; gephyrin; narcolepsy; PSD-95; rat; paradoxical sleep; REM sleep; sleep/wake states; stereology; VAChT; VGAT; VGluT2

Neurons containing the peptide orexin (Orx, also called hypocretin) play a critical role in maintaining wakefulness and associated postural muscle tone, since in their absence or that of the peptide or receptor, narcolepsy with cataplexy occurs in humans and animals (Chemelli et al., 1999; Lin et al., 1999; Peyron et al., 2000; Thannickal et al., 2000; Yamanaka et al., 2003a). The Orx neurons are located within the tuberal hypothalamus, where they are broadly distributed across the lateral hypothalamic area (Broberger et al., 1998; Peyron et al., 1998; Modirrousta et al., 2005; Swanson et al., 2005), a region long known to play an important role in arousal (see, for review, Jones, 2005a). Lying there within the path of the medial forebrain

*Correspondence to: Dr. Barbara E. Jones, Montreal Neurological Institute, McGill University, 3801 University St., Montreal, Quebec, Canada H3A 2B4. E-mail: barbara.jones@mcgill.ca.

bundle (MFB) (Millhouse, 1969; Veening et al., 1982), the Orx neurons have recently been shown to receive inputs from multiple forebrain and brainstem cell groups (Sakurai et al., 2005; Yoshida et al., 2006), which project through the MFB and are involved in sleep/wake state regulation (Jones, 2005a). The sources of afferent input might include the basal forebrain (BF) (Sakurai et al., 2005), which, from lesion, stimulation, and recording studies is known to play diverse roles in sleep/wake state regulation through its different constituent cell groups (Szymusiak et al., 2000; Jones, 2005a,b).

The BF is known particularly for the cholinergic neurons residing there within multiple nuclei and projecting to the cerebral cortex, where they stimulate cortical activation during waking and paradoxical sleep (PS, also called rapid eye movement, REM, sleep; see, for review, Jones, 2004). However, the BF also contains more numerous noncholinergic neurons, including GABAergic and glutamatergic neurons that appear to play different roles in sleep/wake state regulation, including the promotion of slow wave sleep (SWS) or, conversely, waking (Lee et al., 2004; Jones, 2005b). From retrograde tracing studies, we previously found that few cholinergic neurons, but many GABAergic and other unidentified BF neurons, project caudally to the lateral hypothalamus (LH) (Gritti et al., 1994). Most recently, using anterograde transport of biotinylated dextran amine (BDA) together with immunohistochemistry for the vesicular transporter proteins (VTPs), we established that a minor proportion of terminals projecting into the LH from the BF contained the VTP for acetylcholine (ACh, VAChT), whereas a major proportion contained that for GABA (VGAT) and a remaining proportion contained the VTP for glutamate (VGluT2 and not VGluT1 or VGluT3), proving an important glutamatergic in addition to GABAergic contingent of the BF inputs to the LH (Henny and Jones, 2006). We also established in that study that the cholinergic, GABAergic, and glutamatergic projecting neurons were phenotypically distinct, since the VTPs were not colocalized in the same terminals. The BF afferents would thus release ACh, GABA, or glutamate. The aim of the present study was thus to examine if the Orx neurons in the hypothalamus are innervated by BF terminals and, if so, whether they might be selectively or preferentially innervated by cholinergic, glutamatergic, or GABAergic terminals and thereby influenced in a particular manner by BF neurons across the sleep/waking cycle.

Using anterograde transport of 10,000 MW BDA in rats (Henny and Jones, 2006), we examined in the present study the innervation of Orx neurons by neurons of the magnocellular preoptic nucleus (MCPO) and substantia innominata (SI) of the BF cholinergic cell area from where significant hypothalamic as well as neocortical projections originate (Gritti et al., 1994, 1997) and can influence behavioral in addition to cortical components of sleep/wake states (Szymusiak et al., 2000; Jones, 2004, 2005a,b). First, using single or dual-staining, we quantitatively studied and estimated with stereological analysis the distribution of Orx neurons in the hypothalamus and their contact by BDA-labeled terminals in light microscopy. Second, using triple-staining for Orx, BDA, and the VTPs, we quantitatively examined and estimated with stereological analysis the contacts on the Orx neurons by BDA-labeled terminals containing VAChT, VGluT2, or VGAT in fluorescence microscopy. Third, given evidence of prominent VGluT2 and VGAT-containing terminals apposing the Orx neurons, we further studied their contacts by confocal laser scanning microscopy and 3D reconstruction with rotation. Lastly, to ascertain whether such varicosities might form excitatory or inhibitory synapses on the Orx neurons, we similarly examined sections triple-stained for BDA, Orx, and the scaffolding postsynaptic proteins (PSPs), PSD-95 as a marker for asymmetric, glutamatergic synapses (Sheng and Pak, 2000; Sassoe-Pognetto et al., 2003) or gephyrin (Geph) as a marker for symmetric, GABAergic synapses (Pfeiffer et al., 1984; Giustetto et al., 1998; Sassoe-Pognetto and Fritschy, 2000; Sassoe-Pognetto et al., 2000). Using 3D reconstruction with rotation of high-resolution confocal images, we document important glutamatergic and GABAergic BF inputs onto Orx neurons.

MATERIALS AND METHODS

Animals and surgery

All procedures conformed to the guidelines of the Canadian Council on Animal Care and the US NIH and were approved by the McGill University Animal Care Committee.

As previously described in detail (Henny and Jones, 2006), Long Evans rats (200–250 g, Charles River Canada, St. Constant, Quebec, Canada) were anesthetized and placed in a stereotaxic frame (David Kopf Instruments, Tujunga, CA) for surgery. Glass micropipettes (tip diameter 15–25 μm) were back-filled with a 0.5 M NaCl solution containing 2% 10,000 MW BDA (BDA-10,000, Molecular Probes, Eugene, OR). Since previous studies using anterograde as well as retrograde tracing methods showed no evidence for contralateral projections from BF to the posterior hypothalamus (Swanson, 1976; Gritti et al., 1994), bilateral injections of BDA were performed. The pipettes were lowered into the region of the MCPO on each side (from bregma: anterior-posterior (AP), −0.5 mm; lateral (L), ± 2.5 mm; vertical (V), 8.5 mm) (Paxinos and Watson, 1986) with the aid of a micropositioner (Model 660, David Kopf Instruments). Once in the targeted site, microinjection of BDA was performed by iontophoresis (using a Microiontophoresis Dual Current Generator 260, World Precision Instruments (WPI), Sarasota, FL) applying positive current pulses (5–10 μA) in a duty cycle of 1 second (0.5 seconds on, 0.5 seconds off) for a period of 25–30 minutes through a stimulator (Pulsemaster A300, WPI) and stimulus isolation unit (Iso-Flex, A.M.P.I., Jerusalem, Israel).

Rats were maintained for 5 or 6 days with food and water ad libitum and subsequently perfused transcardially under deep sodium pentobarbital anesthesia (100 mg/kg, intraperitoneally, i.p.) with ~500 mL 4% paraformaldehyde fixative solution. The brains were removed and put in a 30% sucrose solution for 2–3 days, after which they were frozen at −50°C and stored at −80° C for subsequent processing.

Immunohistochemistry

Sections were cut using a freezing microtome in 25 μm-thick coronal sections and collected in eight adjacent series at 200-μm intervals through the forebrain, including the magnocellular basal forebrain and the tuberal hypothalamus. To visualize BDA-labeled neurons in the BF as well anterogradely labeled axons in the tuberal hypothalamus, the avidin-biotin-peroxidase complex (ABC) protocol was used with diaminobenzidine (DAB) intensified with Nickel (DAB-Ni). Sections were subsequently counterstained for Nissl substance using Neutral Red.

For the mapping, distribution, and quantitative estimates of Orx+ cells in the hypothalamus, serial sections were incubated overnight with goat (Gt)-Anti-Orx-A (1:500, see Table 1) and stained with DAB following incubation with donkey (Dky) anti-Gt IgG and Gt peroxidase-antiperoxidase (PAP, both from Jackson ImmunoResearch Laboratories, West Grove, PA).

For evaluation of the injection sites, description of BDA-labeled fibers in the tuberal hypothalamus, and examination of the innervation of Orx+ cells in the region, series were processed for dual-staining of BDA using the ABC procedure with DAB-Ni and Orx-A (above) using PAP with alpha-naphthol pyronin B (ANPB, Sigma, St. Louis, MO). Injection sites on one or two sides from nine rats were selected according to their placement in the MCPO and SI (n = 16 cases) for subsequent processing and analysis in peroxidase or fluorescent stained material.

For triple fluorescent staining of Orx with the VTPs (VAChT, VGluT2, or VGAT) and BDA (see Tables 1 and 2), free-floating sections from each series were rinsed for 30 minutes in Trizma saline buffer (TS, 0.1 M, pH 7.4) followed by incubation for 30 minutes with a blocking solution of normal donkey serum (NDS, 6% in TS) containing 0.3% Triton X-100 (TX).

Sections were subsequently coincubated overnight at room temperature with VTP and Orx-A primary antibodies (in TS containing NDS 1% and TX 0.3%). Prior pilot studies determined that incubation in TX 0.3% allowed full penetration of the antibodies and streptavidin, as viewed through the z-axis under epifluorescent and confocal microscopy. The next day sections were incubated for 3 hours in indocarbocyanine (Cy3)- and aminomethylcoumarin acetate (AMCA) or indodicarbocyanine (Cy5)-conjugated secondary antibodies, followed by 3 hours in cyanine (Cy2)-conjugated-streptavidin (SA) for BDA revelation. For triple fluorescent staining of BDA with the PSPs, PSD-95 or Geph, and Orx, the same protocol was used by coincubation with the PSP and Orx antibodies overnight (see Tables 1 and 2).

All sections were mounted out of Trizma water and the mounted sections dehydrated through alcohols, cleared in xylene, and coverslipped with Permount.

Conventional microscopy, tracing, and stereological analysis

Sections were examined under light and epifluorescent microscopy with a Leica DMLB or Nikon E800 microscope equipped with an x-y-z motorized stage, video or digital camera, and filters appropriate for FITC or Cy2, Rhodamine or Cy3, DAPI-AMCA, and/or Cy5 fluorescence. Single as well as composite images were acquired on the Nikon or Leica microscopes using Neurolucida software from MicroBrightField (MBF, Colchester, VT), which was also used for plotting cells and tracing fibers. In light or fluorescent material, cells and varicosities were counted using the Optical Fractionator probe of StereoInvestigator software (MBF) on the Nikon microscope. For tracing or counting, a computer-resident atlas of the rat brain was employed that was developed and applied in our laboratory using standardized procedures for tissue processing. For each application, series of histology sections are matched to appropriate levels of the atlas (at 400-μm intervals) under low magnification (5 or 10× objective). At each level the atlas image is then rotated, if necessary, and the contours adjusted to optimally fit the relevant nuclei of the histology section. In the BF, the number of BDA-labeled cells was counted through the injection site within the MCPO and SI (Gritti et al., 1993; Henny and Jones, 2006). Through the hypothalamus, Orx neurons were plotted and counted through their full distribution across three AP levels (in mm from Interaural (A) zero): ~A6.6, A6.2, and A5.8 (Paxinos and Watson, 1986), and within three contours, the LH, comprising the region lateral to the fornix through which the MFB passes and present at levels ~A6.6, A6.2, and A5.8; the perifornical area (PF), comprising the area surrounding and extending medial to the fornix; and the dorsomedial hypothalamic nucleus (DMH) and present at levels ~A6.2 and ~A5.8 (Veening et al., 1982; Modirrousta et al., 2005). BDA-labeled fibers were plotted and analyzed using the same atlas sections and contours.

For representation of the distribution of the Orx population, Orx+ neurons (stained with DAB) were plotted under brightfield illumination with a 40× objective at three levels (above) using Neurolucida. In the same material, stereological estimates of the total number of Orx+ cells across three levels in the LH, and two levels in the PF and DMH, were obtained using StereoInvestigator. Within the optical fractionator probe, cells were counted with a 60× oil objective (1.40 numerical aperture, NA) using a counting frame of 120 × 120 μm and a sampling grid size of 240 × 240 μm to sample 25% of the x-y area of each nucleus. Within each counting frame or block, all cells whose tops came into focus beneath the surface of the section were counted through a 10-μm dissector height in the z-axis, which corresponded to the average thickness of the mounted (dehydrated, cleared, and coverslipped) sections in this series.

To examine the relationship of BF axons to the Orx neurons in the hypothalamus, BDA-labeled fibers (stained black with DAB-Ni) and Orx+ cell bodies (stained fuchsia with ANPB) were traced under brightfield illumination using the Neurolucida software (MBF). Axons and cell bodies were drawn using a 100× oil objective within contours of the LH, PF, and DMH. Unbiased estimates of the number and proportion of Orx+ neurons receiving contacts from BF

varicosities were obtained in the LH, where both the Orx+ cells and BF varicosities were most numerous, as well as in PF and DMH. An Orx+ cell was considered to be contacted if a BDA + varicosity was seen in direct apposition to the cell, with no obvious space observed between them and at a point where both were located at the approximately same focal plane. Stereological counts were obtained of Orx+ cells that were (Orx+: BDA+) or were not (Orx +:BDA+) contacted by one or more BDA+ varicosities through the LH, PF, and DMH (n = 3). Counts were performed under a 100× oil objective (1.40 NA) at three levels (above) within the LH contour and two levels (above) within PF and DMH contours. Within the optical fractionator probe, a counting frame of 70 × 70 μm was employed with a sampling grid size of 140 × 140 μm so as to sample 25% of the area. Within each counting frame or block, all cells whose tops came into focus beneath the surface of the section were counted through 15 μm in the z-axis, which was the average thickness of the mounted sections in this series.

To examine the relationship of BDA+ terminals containing different VTPs [VTP+] to Orx+ cells, triple-stained sections were viewed under epifluorescent microscopy to determine if BDA + [VAChT+], BDA+ [VGluT2+], or BDA+ [VGAT+] varicosities appeared to come into contact with Orx+ cells stained with AMCA or Cy5 (see Table 2). Additional series were used for stereology in which Orx cells were stained with Cy5 (using the antibody from Gt in combination with anti-VTP antibodies from Rb; Table 2). Unbiased estimates were obtained of the total number and proportion of innervated Orx+ cells that were contacted by each of the BDA+ [VTP+] type of varicosity by counting Orx+:BDA+ [VTP+] along with Orx+:BDA+ [VTP+] cells through three levels of the LH contour in each series (n = 3). In addition, estimates of the total number and proportion of contacting varicosities were computed for each of the BDA+ [VTP+] type of varicosity by using counts of BDA+[VTP+]:Orx+ and BDA+[VTP +]:Orx+ varicosities (n = 3). The presence of BDA+ contacts on the counted cells was assessed online by sequential observation of the material through the different filters at the same focal plane and multiple planes through the z-axis. Counts were performed under a 100μ oil objective (with 1.40 NA) within a counting frame of 70 × 70 μm and using a sampling grid of 120 × 120 μm so as to sample ~33% of the LH area. Within each counting frame or block, all cells whose tops came into focus beneath the surface of the section were counted through 8 μm in the z-axis, which corresponded to the average thickness of the mounted sections in these series.

Confocal microscopy and image processing

Material triple-stained for BDA/VTP/Orx or BDA/PSP/Orx was examined in a Zeiss LSM 510 laser scanning confocal microscope equipped with Argon 488 nm, helium-neon 543 nm, and helium-neon 633 nm lasers for Cy2, Cy3, and Cy5 excitation, respectively. Appropriate filters were used for detection of Cy2 (bandpass 500–530 nm, green), Cy3 (bandpass 565–615 nm, red), and Cy5 (bandpass 697–719 nm, infrared, color-coded in blue). Scanning was performed through a Plan-Apochromat 100× (with 1.4 NA) objective and pinhole size of ~0.8 (0.6–1, Airy Units) for the three channels. Acquisition was performed with the resident LSM 510 software and consisted of stacks of images taken through the z-axis in optical slices of ~0.5 μm for VTPs, or ~0.33 μm for PSPs series. Additional high-resolution stack images (optical slices of ~0.05–0.1 μm) were acquired for the PSP series.

Rendered 3D views of the stacks were obtained using the fluorescence rendering mode from the image software Volocity 3.7 (Improvision, Lexington, MA, www.improvision.com), which provides a semitransparent 3D view of the different elements based on the degree of intensity of each voxel (i.e., the more intense, the less transparent). The different elements could then be examined simultaneously and interactively from different angles and magnifications. Thus, varicosities could be judged to be in contact with a postsynaptic cell or process, as assessed by the absence of space between the presynaptic and postsynaptic element from any of the angles observed (Wouterlood et al., 2002). High-resolution image stacks (see above) were analyzed

in the fluorescent rendering mode as well as in the isosurface rendering mode, which provides a 3D solid, nontransparent view of the element surface. Channels in which the signal was low or the noise was relatively high were restored using a deconvolution procedure (iterative restoration in Volocity).

Adjustment for brightness and contrast for all pictures, in addition to adjustment of tonal range for each individual RGB channel ("Adjust/Levels" command in Photoshop) for fluorescent images were performed with Adobe Photoshop Creative Suite edition (Adobe System, San Jose, CA). Figure preparation and final montage were done with Adobe Illustrator Creative Suite edition.

RESULTS

BDA injection site and anterograde labeling in the hypothalamus

Iontophoretic application of BDA-10,000 into the region of the MCPO-SI (Fig. 1A) on two sides in nine rats produced small and well-restricted, spherical injection sites (Fig. 1B) of <500 μm diameter and containing (some ~1,400) labeled nerve cell bodies, as previously described (Henny and Jones, 2006). Injection sites were positioned primarily within the MCPO and SI (in n = 16 cases selected for analysis), where ~90% and ~6% of labeled cells were located, respectively. BDA-labeled fibers coursed through the MFB to reach the tuberal hypothalamus, where multiple neurons, particularly in the LH, were contacted by varicosities (Fig. 1C) (Henny and Jones, 2006).

Number and distribution of Orx+ neurons in the hypothalamus

The distribution and numbers of Orx+ neurons were examined in PAP (DAB)-stained material. Orx+ cells were distributed across the tuberal hypothalamus in moderate numbers from rostral to caudal levels (~A6.6, A6.2, and A5.8, Fig. 2). Although most concentrated in the area immediately surrounding and dorsal to the fornix, cells were distributed through the LH, PF, and DMH. According to stereological estimates of total numbers of cells (mean ± SEM, n = 3), ~1,800 Orx+ cells were located within the LH, ~500 in the PF, and ~900 in the DMH with a total of ~3,200 neurons per side (Table 3). The proportions of Orx neurons were thus ~56% in the LH, ~15% in the PF, and ~29% in the DMH contours as delineated here.

BDA-labeled axons in relation to Orx+ neurons

The relation of BF axon terminals to Orx cells was examined in material dual-stained using peroxidase for BDA (in black with DAB-Ni following ABC procedure) and Orx (in fuchsia with ANPB following PAP procedure) (n = 7, Fig. 3). Multiple BDA-labeled fibers were evident in the regions where Orx+ cell bodies and proximal dendrites were present, particularly in the LH (Fig. 3A). Moreover, BDA-labeled axonal boutons en passant (Fig. 3B′) or boutons terminaux (Fig. 3B′, B″) appeared to contact Orx+ cell bodies as well as dendrites. In tracings of all BDA+ fibers along with Orx+ cells at high magnification using Neurolucida, multiple fine collaterals of the coarse fibers within the MFB appeared to extend dorsally and medially to reach Orx+ neurons within the central and dorsal regions of the LH (Fig. 3C, level A6.0, approximately intermediate to those seen in Fig. 2B,C). Here, BDA-labeled varicosities appeared to contact Orx+ soma or proximal dendrites in the LH (Fig. 3D′,D″,D‴). Some BDA-labeled fibers also extended medially to reach into the PF or DMH, although these were few in number. As determined by stereological analysis, the proportion of Orx+ neurons that were contacted by at least one BDA+ varicosity (Orx+:BDA+) within the LH, PF, and DMH, was estimated to be ~41%, ~11%, and ~9%, respectively (Table 3). Overall, ~28% of the total population of Orx+ neurons was contacted by BF axonal varicosities.

Given that the maximal incidence of Orx+ neurons (above), subsequent analyses of the BF innervation contacted occurred in the LH and that the majority of were focused on the Orx+ neurons within the contour of Orx+ neurons were also contained within the LH the LH.

VAChT, VGluT2, and VGAT in BDA-labeled varicosities in relation to Orx+neurons in the LH

To determine if BF terminals contacting Orx neurons are cholinergic, glutamatergic, or GABAergic, sections that were triple-stained for BDA (with Cy2), the VTPs (VAChT, VGluT2, or VGAT with Cy3), and Orx-A (with AMCA or Cy5) were examined under epifluorescent microscopy (see number of cases, n, for each series in Table 2). In these sections, sparse VAChT+ varicosities were evident (Fig. 4A″), whereas multiple VGluT2+ (Fig. 4B″) and VGAT+ (Fig. 4C″) varicosities were present in the vicinity of the Orx+ neurons. BDA+ [VAChT+] (Fig. 4A‴), BDA+ [VGluT2+] (Fig. 4B‴), and BDA+ [VGAT+] (Fig. 4C‴) BF axons were all present in the immediate surround of the Orx+ neurons as well. However, only BDA+ [VGluT2+] (Fig. 4B‴) and BDA+ [VGAT+] varicosities (Fig. 4C‴) appeared to contact the Orx+ neurons in substantial numbers.

Stereological estimates of contacts between VAChT+, VGluT2+, or VGAT+ BDA-labeled varicosities and Orx+ neurons in the LH

To determine the proportions of Orx+ neurons innervated by cholinergic, glutamatergic, or GABAergic BF axon terminals, stereological analysis was used for estimation of the total numbers of Orx+ neurons contacted by each of the BDA+ [VTP+] types of varicosities in the LH through the three levels studied (~A6.6, A6.2, and A5.8, n = 3 cases, Table 4). In the VAChT series, less than 4% of the Orx+:BDA+ neurons were contacted by BDA+ [VAChT+] varicosities. In the VGluT2 series, ~31% of the Orx+:BDA+ neurons were contacted by BDA + [VGluT2+] varicosities. In the VGAT series, ~67% of the Orx+:BDA+ neurons were contacted by BDA+ [VGAT+] varicosities.

The number of BDA+ [VTP+] varicosities contacting Orx+ neurons (BDA+ [VTP+]:Orx+) was also determined (n = 3, Table 4). As estimated from each series, the proportions of varicosities in contact with Orx+ neurons were, respectively: ~2% for BDA+ [VAChT+], ~17% for BDA+ [VGluT2+], and ~58% for BDA+ [VGAT+] varicosities. Across series, the numbers of terminals detected per Orx+ cell were: one for BDA+ [VAChT+], one to two for BDA+ [VGluT2+], and one to four for BDA+ [VGAT+] varicosities. Given the minimal number of contacts by BDA+ [VAChT+] varicosities and the substantial number of contacts by BDA+ [VGluT2+] and BDA+ [VGAT+] varicosities on the Orx+ neurons, confocal analysis was pursued for the latter terminals.

Confocal analysis of VGluT2 or VGAT inside and of PSD-95 or gephyrin opposite BDA +terminals on Orx+neurons

To examine in detail the nature of the BDA+ contacts observed on Orx+ neurons, confocal microscopic analysis was performed on material triple-stained for BDA (with Cy2), Orx (with Cy5 or Cy3) and markers for the presynaptic, VTP (VGluT2 or VGAT with Cy3) or postsynaptic, PSP (PSD-95 or Geph with Cy5) (see Table 2 for number of cases processed and examined for each series). Confocal images were further viewed using 3D reconstruction and rotation with magnification to confirm that the pre- and postsynaptic elements were in contact through three spatial axes.

In series triple-stained for BDA, VGluT2, and Orx, the Orx+ neurons were seen to be surrounded by numerous VGluT2+ varicosities. In this material, many BDA-labeled VGluT2 + varicosities were apposed to Orx+ soma (Fig. 5A) or proximal dendrites (not shown). As judged from examination and rotation of 3D images from such cases, the BDA+ [VGluT2+]

varicosity appeared to be in contact with the Orx+ cell, since no space could be observed between the two (Fig. 5A, small images) with rotation through three axes.

In series triple-stained for BDA, PSD-95, and Orx, staining for PSD-95 appeared punctate and could be seen on the surface of Orx+ neurons (Fig. 5B). In some BDA+: Orx+ contacts (Fig. 5B), PSD-95+ puncta could be detected opposite the BDA+ varicosity and associated with the Orx+ cell (Fig. 5B, small images). From 93 acquired images of appositions (from n = 3 cases), 74 BDA+:Orx+ contacts (~80%) were confirmed in rotated and magnified 3D images, and 16 of these, 21.6%, showed staining for PSD-95 opposite the BDA+ varicosity and associated with the Orx+ cell.

To further assess the spatial relationship among the BDA+ terminals, PSD-95+ puncta, and Orx+ cells, image stacks with high z-axis resolution (0.05–0.10 μm optical slices) were acquired of 23 appositions (from n = 3 cases) and analyzed in 3D rotations. Contacts were confirmed between BDA+ varicosities and Orx+ neurons, as shown from three different, orthogonal 3D angles of semitransparent fluorescence images (Fig. 6A1,B1,C1). PSD-95+ profiles were observed in apposition to BDA+ varicosities (Fig. 6A2,B2,C2) and in association with the surface of Orx+ neurons (Fig. 6A3,B3), being localized between BDA+ and Orx+ elements (Fig. 6A4,B4). Opaque isosurface rendering of the three elements further evidenced the localization of PSD-95+ puncta, which appear tucked in or hidden between the BDA+ varicosity and the Orx+ neuron (Fig. 6A5,B5,C5).

In series triple-stained for BDA, VGAT, and Orx, Orx+ neurons were also seen to be surrounded by VGAT+ varicosities. Many BDA-labeled VGAT+ varicosities were in close apposition to Orx+ soma or dendrites (Fig. 5C). As judged from the rotated and magnified 3D images of such cases, the BDA+ [VGAT+] varicosity was in contact with the Orx+ cell (Fig. 5C, small images) through three axes.

In series triple-stained for BDA, Geph, and Orx, Geph staining (Cy5) appeared punctate, generally in larger puncta than PSD-95 and frequently associated with Orx+ soma and dendrites (Fig. 5D). In multiple BDA+:Orx+ contacts (Fig. 5D), Geph+ puncta were seen facing the BDA+ varicosity and associated with the Orx+ cell (Fig. 5D, top small images), such that they appeared to be located between the terminal and cell in merged images (Fig. 5D, lower small image). From 112 acquired images of appositions (from n = 3 cases), 93 BDA+:Orx+ contacts (>80%) were confirmed in rotated and magnified 3D images, and 44 or 47.3% showed Geph + puncta between the BDA+ varicosity and the Orx+ cell.

For further analysis, image stacks with high z-axis resolution (0.05–0.10 μm optical slices) were acquired of 19 (from n = 3 cases) BDA, Geph, and Orx appositions and examined. Contacts were seen between BDA+ varicosities and Orx+ neurons, as evidenced from 3D orthogonal views (Fig. 6D1,E1,F1). Geph+ profiles were observed in apposition to BDA+ varicosities (Fig. 6E2,F2) and in association with the surface of Orx+ neurons (Fig. 6D3,E3,F3), located between BDA+ and Orx+ elements (Fig. 6E4,F4). Opaque isosurface rendering of the three elements evidenced the localization of Geph+ puncta between the BDA + varicosity and the Orx+ neuron (Fig. 6D5,E5,F5).

DISCUSSION

The present study presents qualitative and quantitative evidence that Orx neurons are innervated by afferents from the BF cholinergic cell area. Yet from this cholinergic cell area the afferents were predominantly comprised of noncholinergic terminals. Numerous glutamatergic and GABAergic varicosities contacted Orx neurons in the LH and could thus respectively exert excitatory and inhibitory influences on their activity during wake and sleep states.

BF projections to Orx neurons

We show here that anterogradely labeled fibers from the MCPO-SI of the BF cholinergic cell area extend into the region of the Orx cells in the tuberal hypothalamus. As shown and discussed in our previous study (Henny and Jones, 2006), the fibers reached the caudal hypothalamus through the ventrolateral portion of the MFB, which has long been known to carry fibers from this forebrain area (Swanson, 1976; Veening et al., 1982; Grove, 1988). From this component, collaterals fan out through the LH and extend dorsomedially, although less numerously, through the PF and sparsely into the DMH.

We estimated here using stereology that Orx neurons are most numerous within the LH, numbering ~1,800, less numerous within the PF, numbering ~500, and intermediate in the DMH numbering ~900 for a total of ~3,200 neurons per side. The total number (in Long Evans rats) is similar to that previously estimated by us as ~3,400 Orx+ neurons per side (in Wistar rats) (Modirrousta et al., 2005) and to one other published number estimated by stereological analysis as ~2900 Orx+ neurons per side (in Wistar rats) (Allard et al., 2004). According to conventional delineation as the region lateral to the fornix through which the MFB fiber systems travel, >50% (or ~1,800) of the Orx cells are located in the LH.

We show here that BF terminals, which would originate from a relatively small number of caudally projecting cells in the MCPO-SI labeled by the BDA injections, contact a significant proportion (~28%) of all Orx+ cells. This input was topographically arranged, as the proportions of Orx+ cells contacted were substantial (~41%) in the LH and small in the more medial PF (~11%) and DMH (~9%). Notably, from similar injection sites, BF terminals contact only ~15% of the total LH cell population (estimated at ~50,000 through the tuberal hypothalamus) (Henny and Jones, 2006), suggesting a selective enrichment of BF terminals upon the Orx neurons relative to all other chemically unidentified neurons of the LH. According to a recent extensive survey of afferents to the Orx neurons using both anterograde and retrograde tracing (Yoshida et al., 2006), the overall proportion of Orx neurons contacted by BF afferents (~28%, from the present study) would be comparable to that originating from the adjacent ventrolateral preoptic area (31%). In the former work, the BF was not considered to be among the major afferent sources to the Orx neurons, although it contained a moderate number of afferent cells (Yoshida et al., 2006). In that study the afferents were identified by injections of retrograde tracers into the region where the Orx+ neurons are most concentrated, immediately surrounding the fornix within the dorsal PF, the lateral DMH, and the dorsomedial region of the LH, and thus highlighted major sources of input from the more medial basal telencephalic afferent systems. From our present and previous (Gritti et al., 1994; Henny and Jones, 2006), as well as other early tracing studies (Swanson, 1976; Veening et al., 1982; Grove, 1988), the MCPO-SI would fit within a lateral-to-medial as well as ventral-to-dorsal topographically organized system of fibers coursing within the MFB and serving as afferents to the hypothalamus and, notably, as the present results indicate, the Orx neurons therein.

Predominant innervation by noncholinergic, glutamatergic, and GABAergic BF terminals of Orx neurons

In the LH, of the total number of Orx neurons contacted by BF axonal varicosities (~41%, see above), only a minimal proportion (~4%) was innervated by cholinergic varicosities, whereas the major proportion was innervated by glutamatergic or GABAergic varicosities. Similarly, only 2% of the varicosities on Orx~ cells were VAChT~ in this material. These results are in line with our previous study showing that cholinergic BF terminals in the LH comprise less than 10%, whereas glutamatergic and GABAergic terminals comprise the vast majority of the BF terminals in the LH (Henny and Jones, 2006). These are not in agreement with the recent results of Sakurai et al. (2005) using a transgene for a tetanus toxin tracer (tetanus toxin C fragment fused to green fluorescent protein, TTC::GFP), which is believed to be transported

transynaptically and retrogradely, linked to an *orexin* promoter together with fluorescent staining for choline acetyltransferase (ChAT). In those studies, essentially all retrogradely labeled neurons in the cholinergic cell area of the BF were judged to be immunostained for ChAT. We recognize the possibility that the TTC::GFP tracer could be taken up by terminals on distal dendrites that were not evident in our fluorescent material. On the other hand, previous results from our lab and from other groups utilizing retrograde transport of traditional tracers also found minimal proportions of descending projections from cholinergic BF neurons (<5%) to the brainstem or hypothalamus and the region of the Orx cell bodies and dendrites (Grove, 1988; Semba et al., 1989; Gritti et al., 1994; Bayer et al., 1999). As discussed by Sakurai et al. (2005), retrograde labeling by TTC::GFP could be due to transynaptic transport along with retrograde transport that could result in labeling of a large number and proportion of cholinergic BF cells as higher-order afferent neurons. Such an indirect, multisynaptic influence of cholinergic BF neurons upon Orx neurons might be expected to exist as a feedback on the Orx neurons that project into the region of the cholinergic cells (Espana et al., 2005) and would exert an excitatory effect through Orx on the cholinergic neurons (Eggermann et al., 2001). On the other hand, from electrophysiological studies it appears that cholinergic input can have an important influence on Orx neurons, since cholinergic agonists can depolarize and excite the Orx neurons (Bayer et al., 2005; Sakurai et al., 2005). Although the BF cholinergic cells may participate in this influence, the pontomesencephalic cholinergic neurons likely play a more dominant role, given previous evidence of their more substantial projections into the region of the Orx cells (Ford et al., 1995; Bayer et al., 1999).

We found that a substantial proportion of BF-innervated Orx neurons were contacted by VGluT2 containing BDA-labeled terminals (~31%), and that a substantial proportion of the BDA-labeled terminals contacting Orx neurons were VGluT2+ (~17%). Glutamate has been shown to depolarize Orx neurons through both NMDA and AMPA receptors in vitro (Li et al., 2002; Yamanaka et al., 2003b). Orx neurons have been described as receiving a relatively high density of VGluT2+ varicosities and asymmetric, presumed excitatory synapses (Horvath and Gao, 2005). From the present results, one source of these multiple glutamatergic inputs can be attributed to BF neurons.

The major proportion of BF-innervated Orx neurons were contacted by VGAT containing BDA-labeled terminals (~67%), and a major proportion of the BDA-labeled varicosities were VGAT+ (~58%), indicating that GABAergic BF neurons can have a potent influence on Orx neurons. GABA has been shown to hyperpolarize and inhibit Orx neurons that are otherwise spontaneously active in vitro (Li et al., 2002; Eggermann et al., 2003; Yamanaka et al., 2003b). Interestingly, Orx neurons are considered to have a relatively sparse GABAergic input, particularly in relation to the glutamatergic input, with a ratio of inhibitory to excitatory synapses estimated as 1 to 10 (Horvath and Gao, 2005). In light of the latter results, it would appear that the BF GABAergic neurons may play a particularly important role in providing this inhibitory input and influence to the Orx cells.

BF glutamatergic and GABAergic synaptic input onto Orx neurons

We confirmed by confocal laser scanning microscopy and 3D image rendering and rotation that BDA-labeled BF varicosities appeared to contact Orx neurons in the LH. By continuous rotation through three axes, we were thus able to establish for large numbers of varicosities that there appeared to be no space between the varicosity and the Orx+ cell. Such confirmation has been considered by others to represent strong evidence for synaptic contacts (Wouterlood et al., 2002). Yet it is well recognized that only the resolution of the electron microscope provides absolute proof of such contacts by presynaptic elements with postsynaptic targets.

More specific evidence is provided for the synaptic nature of glutamatergic and GABAergic terminals by the presence of the presynaptic vesicular transporters. VGluT2 and VGAT, which

were demonstrated in the BDA-labeled varicosities apposed to Orx cells, confer the capacity to release glutamate and GABA and are concentrated in the presynaptic terminal at asymmetric and symmetric synapses, respectively (Gilmor et al., 1996; Chaudhry et al., 1998; Bellocchio et al., 2000; Takamori et al., 2000; Fremeau et al., 2001, 2004; Gualix et al., 2003).

Lastly, we show that in confirmed contacts of BDA-labeled varicosities with Orx cells, postsynaptic proteins of PSD-95 and Geph are situated facing the varicosity and in association with the Orx+ cell. Similar to proportions of BDA-labeled varicosities ostensibly contacting Orx+ neurons that were VGluT2+ and VGAT+ (above), the proportions of confirmed contacts by BDA-labeled varicosities on Orx+ neurons that showed PSD-95 or Geph puncta between the terminal and cell were ~22% and ~47%, respectively. Postsynaptic proteins, PSD-95, and Geph are constituent parts of the postsynaptic scaffolding of asymmetric, excitatory (Sheng and Pak, 2000), and symmetric inhibitory synapses (Sassoe-Pognetto and Fritschy, 2000), respectively. At excitatory synapses, PSD-95 colocalizes by direct and indirect association with NMDA and AMPA receptors (Sassoe-Pognetto et al., 2003). At inhibitory synapses, Geph is colocalized with the most common synaptic subtypes of $GABA_A$ receptors and is suggested to participate in their anchoring to the postsynaptic membrane (Sassoe-Pognetto et al., 1995; Giustetto et al., 1998). The location of postsynaptic proteins sandwiched between pre-synaptic and postsynaptic elements has been considered strong evidence for synaptic contacts in 3D rendered confocal images (Wouterlood et al., 2003). We thus believe that the present results showing both pre- and postsynaptic elements for glutamatergic and GABAergic synapses in association with BDA-labeled terminals contacting Orx neurons provide compelling evidence for BF glutamatergic and GABAergic synaptic input to the Orx cells.

Functional significance of the cholinergic, glutamatergic, and GABAergic BF input to Orx neurons

Orx neurons play a key role in stimulating and maintaining arousal by excitatory influences on multiple systems, including the cerebral cortex, hypothalamic, and brainstem arousal systems, as well as sympathetic and motor circuits in the spinal cord (Peyron et al., 1998; van den Pol, 1999; Saper et al., 2001; Taheri et al., 2002; Krout et al., 2003; Siegel, 2004; Jones and Muhlethaler, 2005; Sakurai, 2005). As now shown by recent studies, they are in turn influenced by afferent input from multiple fore-brain and brainstem systems (Sakurai et al., 2005; Yoshida et al., 2006). Here we show that neurons of the BF cholinergic cell area, which themselves are importantly involved in regulating sleep/wake states, contribute significantly to that afferent input. The BF input was particularly dense onto the Orx neurons in the LH, which despite claims of being selectively activated with reward seeking (Harris et al., 2005), have also clearly been shown to discharge and express c-Fos in association with simple waking, arousal, or stress (Espana et al., 2003; Lee et al., 2005a; Mileykovskiy et al., 2005; Modirrousta et al., 2005).

In contrast to recent claims (above, Sakurai et al., 2005), the cholinergic BF cells appear to contribute minimally to the innervation of the Orx neurons in the LH. Cholinergic BF neurons discharge in a manner (Lee et al., 2005b) that differs fundamentally from that of recently identified Orx neurons across sleep/wake states (Lee et al., 2005a). Whereas cholinergic neurons discharge maximally during both waking and PS in association with cortical activation, Orx neurons discharge maximally during waking in association with movement and muscle tone and cease firing during PS sleep with muscle atonia (Jones, 2005b). It is thus not surprising that Orx neurons are not under the direct control of cholinergic BF neurons. To the contrary, the silence of Orx neurons during PS sleep is the condition under which cholinergic neuronal discharge stimulates cortical activation in association with the muscle atonia of that state.

The Orx neurons receive a substantial glutamatergic input from BF neurons, indicating that these glutamatergic neurons can exert a significant excitatory influence on Orx cells. In single

unit recording studies, many noncholinergic BF neurons have been identified that discharge maximally during active waking and are virtually silent during sleep, including PS sleep (Szymusiak and McGinty, 1986b; Lee et al., 2004, 2005b). The discharge of these neurons is positively correlated with postural muscle tonus or neck electromyographic (EMG) activity (Lee et al., 2004), like that of the Orx neurons (Jones, 2005b; Lee et al., 2005b). We propose that such noncholinergic neurons are glutamatergic and could facilitate behavioral arousal in part by exciting the Orx cells.

The major input to the Orx neurons from BF is GABAergic. Given the purportedly small inhibitory input relative to excitatory input onto Orx neurons (Horvath and Gao, 2005), this GABAergic input from BF neurons might be of critical importance in inhibiting the discharge of Orx neurons during periods of behavioral quiescence, sleep, and/or muscle atonia (Lee et al., 2005a). Although we have identified GABAergic neurons that discharge in association with cortical activation (Manns et al., 2000), we propose that the innervation of the Orx neurons originates from the particular GABAergic BF neurons that are active during sleep (Modirrousta et al., 2004) and discharge during SWS and/or PS sleep in negative correlation with muscle tonus or EMG (Szymusiak and McGinty, 1986b; Manns et al., 2000; Lee et al., 2004; Jones, 2005b).

Orexin has been attributed a particularly important role in maintaining arousal, since in its absence in knockout mice or that of its receptor in dogs or Orx neurons in humans, narcolepsy occurs (Chemelli et al., 1999; Lin et al., 1999; Peyron et al., 2000; Thannickal et al., 2000; Hara et al., 2001). In humans, narcolepsy is characterized by excessive daytime sleepiness, short onset of REM sleep, and/or loss of postural muscle tone, known as cataplexy. Accordingly, the excitation of Orx neurons by presumed wake-active, glutamatergic BF neurons could normally serve to prevent sleep onset and loss of postural muscle tone, whereas the inhibition of Orx neurons by presumed sleep-active GABAergic BF neurons could promote sleep onset and the loss of postural muscle tone. It could be due in part to withdrawal of the major BF GABAergic input to Orx neurons that neurotoxic lesions of the BF result in a severe disruption of SWS and PS (Szymusiak and McGinty, 1986a). Moreover, chemical stimulation of the BF with cholinergic agonists or agents exciting cholinergic neurons can elicit PS with atonia in cats and rats (Hernandez-Peon et al., 1963; Cape et al., 2000; Jones, 2004) and/or cataplexy in dogs (Nishino et al., 1995). Cholinergic agonists and ACh, which is released in the BF maximally during PS (Vazquez and Baghdoyan, 2001), could excite noncholinergic, presumed GABAergic BF neurons (Fort et al., 1998; Wu et al., 2000), including those that innervate the Orx neurons and thereby elicit PS and/or muscle atonia.

In conclusion, the present study reveals an important glutamatergic and GABAergic input to Orx neurons from BF neurons. Glutamatergic BF neurons can excite Orx neurons to stimulate behavioral arousal and waking. GABAergic BF neurons can inhibit Orx neurons to diminish behavioral arousal along with muscle tone and thereby promote sleep, including PS with muscle atonia.

Acknowledgements

We thank Robert H. Edwards and Robert T. Fremeau (Departments of Neurology and Physiology, University of California San Francisco School of Medicine, San Francisco, CA) for kindly supplying the antibody for VGluT2. We thank Lynda Mainville for excellent technical assistance, and Mandana Modirrousta for contributions to the study of the Orx cell population.

Grant sponsors: Canadian Institutes of Health Research; Grant number: CIHR 13458; Grant sponsor: U.S. National Institutes of Health (NIH); Grant number: RO1 MH-60119-01A.

Abbreviations

ABC
Avidin-biotin-peroxidase complex

ac
Anterior commissure

AHA
Anterior hypothalamic area

AMCA
Aminomethylcoumarin acetate

ANPB
Alpha-naphthol pyronin B

Arc
Arcuate nucleus

BDA
Biotinylated dextran amine

BF
Basal forebrain

cp
Cerebral peduncle

Cy2
Cyanine

Cy3
Indocarbocyanine

Cy5
Indodicarbocyanine

DAB
Diaminobenzidine

DAB-Ni
Nickel-intensified diaminobenzidine

DMH
Dorsomedial hypothalamic nucleus

f
Fornix

FS
Fundus striatum

Geph
Gephyrin

ic
Internal capsule

LH
Lateral hypothalamus

LPO
Lateral preoptic area

MCPO
Magnocellular preoptic nucleus

MFB
Medial forebrain bundle

MPO
Medial preoptic nucleus

mt
Mammillothalamic tract

oc
Optic chiasm

Orx
Orexin or hypocretin

ot
Optic tract

Pe
Periventricular hypothalamic nucleus

PF
Perifornical area

Pir
Piriform cortex

PSD-95
95-kD postsynaptic density protein

PSP
Postsynaptic protein

SI
Substantia innominata

SO
Supraoptic nucleus

STh
Subthalamic nucleus

VAChT
Vesicular transporter for acetylcholine

VGAT
Vesicular transporter for GABA

VGluT2
Vesicular transporter for glutamate 2

VMH

Ventromedial hypothalamic nucleus

VTP

Vesicular transporter protein

ZI

Zona incerta

LITERATURE CITED

Allard JS, Tizabi Y, Shaffery JP, Trouth CO, Manaye K. Stereological analysis of the hypothalamic hypocretin/orexin neurons in an animal model of depression. Neuropeptides 2004;38:311–315. [PubMed: 15464197]

Bayer L, Risold PY, Griffond B, Fellmann D. Rat diencephalic neurons producing melanin-concentrating hormone are influenced by ascending cholinergic projections. Neuroscience 1999;91:1087–1101. [PubMed: 10391486]

Bayer L, Eggermann E, Serafin M, Grivel J, Machard D, Muhlethaler M, Jones BE. Opposite effects of noradrenaline and acetylcholine upon hypocretin/orexin versus melanin concentrating hormone neurons in rat hypothalamic slices. Neuroscience 2005;130:807–811. [PubMed: 15652980]

Bellocchio EE, Reimer RJ, Fremeau RT Jr, Edwards RH. Uptake of glutamate into synaptic vesicles by an inorganic phosphate transporter. Science 2000;289:957–960. [PubMed: 10938000]

Broberger C, De Lecea L, Sutcliffe JG, Hokfelt T. Hypocretin/orexin-and melanin-concentrating hormone-expressing cells form distinct populations in the rodent lateral hypothalamus: relationship to the neuropeptide Y and agouti gene-related protein systems. J Comp Neurol 1998;402:460–474. [PubMed: 9862321]

Cape EG, Manns ID, Alonso A, Beaudet A, Jones BE. Neurotensin-induced bursting of cholinergic basal forebrain neurons promotes gamma and theta cortical activity together with waking and paradoxical sleep. J Neurosci 2000;20:8452–8461. [PubMed: 11069953]

Chaudhry FA, Reimer RJ, Bellocchio EE, Danbolt NC, Osen KK, Edwards RH, Storm-Mathisen J. The vesicular GABA transporter, VGAT, localizes to synaptic vesicles in sets of glycinergic as well as GABAergic neurons. J Neurosci 1998;18:9733–9750. [PubMed: 9822734]

Chemelli RM, Willie JT, Sinton CM, Elmquist JK, Scammell T, Lee C, Richardson JA, Williams SC, Xiong Y, Kisanuki Y, Fitch TE, Nakazato M, Hammer RE, Saper CB, Yanagisawa M. Narcolepsy in orexin knockout mice: molecular genetics of sleep regulation. Cell 1999;98:437–451. [PubMed: 10481909]

Eggermann E, Serafin M, Bayer L, Machard D, Saint-Mleux B, Jones BE, Muhlethaler M. Orexins/hypocretins excite basal forebrain cholinergic neurones. Neuroscience 2001;108:177–181. [PubMed: 11734353]

Eggermann E, Bayer L, Serafin M, Saint-Mleux B, Bernheim L, Machard D, Jones BE, Muhlethaler M. The wake-promoting hypocretinorexin neurons are in an intrinsic state of membrane depolarization. J Neurosci 2003;23:1557–1562. [PubMed: 12629156]

Espana RA, Valentino RJ, Berridge CW. Fos immunoreactivity in hypocretin-synthesizing and hypocretin-1 receptor-expressing neurons: effects of diurnal and nocturnal spontaneous waking, stress and hypocretin-1 administration. Neuroscience 2003;121:201–217. [PubMed: 12946712]

Espana RA, Reis KM, Valentino RJ, Berridge CW. Organization of hypocretin/orexin efferents to locus coeruleus and basal forebrain arousal-related structures. J Comp Neurol 2005;481:160–178. [PubMed: 15562511]

Ford B, Holmes C, Mainville L, Jones BE. GABAergic neurons in the rat pontomesencephalic tegmentum: codistribution with cholinergic and other tegmental neurons projecting to the posterior lateral hypothalamus. J Comp Neurol 1995;363:177–196. [PubMed: 8642069]

Fort P, Khateb A, Serafin M, Muhlethaler M, Jones BE. Pharmacological characterization and differentiation of non-cholinergic nucleus basalis neurons in vitro. Neuroreport 1998;9:1–5. [PubMed: 9592037]

Fremeau RT Jr, Troyer MD, Pahner I, Nygaard GO, Tran CH, Reimer RJ, Bellocchio EE, Fortin D, Storm-Mathisen J, Edwards RH. The expression of vesicular glutamate transporters defines two classes of excitatory synapse. Neuron 2001;31:247–260. [PubMed: 11502256]

Fremeau RT Jr, Voglmaier S, Seal RP, Edwards RH. VGLUTs define subsets of excitatory neurons and suggest novel roles for glutamate. Trends Neurosci 2004;27:98–103. [PubMed: 15102489]

Gilmor ML, Nash NR, Roghani A, Edwards RH, Yi H, Hersch SM, Levey AI. Expression of the putative vesicular acetylcholine transporter in rat brain and localization in cholinergic synaptic vesicles. J Neurosci 1996;16:2179–2190. [PubMed: 8601799]

Giustetto M, Kirsch J, Fritschy JM, Cantino D, Sassoe-Pognetto M. Localization of the clustering protein gephyrin at GABAergic synapses in the main olfactory bulb of the rat. J Comp Neurol 1998;395:231–244. [PubMed: 9603375]

Gritti I, Mainville L, Jones BE. Codistribution of GABA- with acetylcholine-synthesizing neurons in the basal forebrain of the rat. J Comp Neurol 1993;329:438–457. [PubMed: 8454735]

Gritti I, Mainville L, Jones BE. Projections of GABAergic and cholinergic basal forebrain and GABAergic preoptic-anterior hypothalamic neurons to the posterior lateral hypothalamus of the rat. J Comp Neurol 1994;339:251–268. [PubMed: 8300907]

Gritti I, Mainville L, Mancia M, Jones BE. GABAergic and other non-cholinergic basal forebrain neurons project together with cholinergic neurons to meso- and iso-cortex in the rat. J Comp Neurol 1997;383:163–177. [PubMed: 9182846]

Grove EA. Efferent connections of the substantia innominata in the rat. J Comp Neurol 1988;277:347–364. [PubMed: 2461973]

Gualix J, Gomez-Villafuertes R, Diaz-Hernandez M, Miras-Portugal MT. Presence of functional ATP and dinucleotide receptors in glutamatergic synaptic terminals from rat midbrain. J Neurochem 2003;87:160–171. [PubMed: 12969263]

Hara J, Beuckmann CT, Nambu T, Willie JT, Chemelli RM, Sinton CM, Sugiyama F, Yagami K, Goto K, Yanagisawa M, Sakurai T. Genetic ablation of orexin neurons in mice results in narcolepsy, hypophagia, and obesity. Neuron 2001;30:345–354. [PubMed: 11394998]

Harris GC, Wimmer M, Aston-Jones G. A role for lateral hypothalamic orexin neurons in reward seeking. Nature 2005;437:556–559. [PubMed: 16100511]

Henny P, Jones BE. Vesicular glutamate (VGluT), GABA (VGAT), and acetylcholine (VAChT) transporters in basal forebrain axon terminals innervating the lateral hypothalamus. J Comp Neurol 2006;496:453–467. [PubMed: 16572456]

Hernandez-Peon R, Chavez-Ibarra G, Morgane PJ, Timo-Iaria C. Limbic cholinergic pathways involved in sleep and emotional behavior. Exp Neurol 1963;8:93–111.

Horvath TL, Gao XB. Input organization and plasticity of hypocretin neurons: possible clues to obesity's association with insomnia. Cell Metab 2005;1:279–286. [PubMed: 16054072]

Jones BE. Activity, modulation and role of basal forebrain cholinergic neurons innervating the cerebral cortex. Prog Brain Res 2004;145:157–169. [PubMed: 14650914]

Jones, BE. Basic mechanisms of sleep-wake states. In: Kryger, MH.; Roth, T.; Dement, WC., editors. Principles and practice of sleep medicine. 4. Philadelphia: Elsevier Saunders; 2005a. p. 136-153.

Jones BE. From waking to sleeping: neuronal and chemical substrates. Trends Pharmacol Sci 2005b; 26:578–586. [PubMed: 16183137]

Jones, BE.; Muhlethaler, M. Modulation of cortical activity and sleep-wake state by hypocretin/orexin. In: de Lecea, L.; Sutcliffe, JG., editors. The hypocretins: integrators of physiological systems. New York: Springer; 2005. p. 289-301.

Krout KE, Mettenleiter TC, Loewy AD. Single CNS neurons link both central motor and cardiosympathetic systems: a double-virus tracing study. Neuroscience 2003;118:853–866. [PubMed: 12710992]

Lee MG, Manns ID, Alonso A, Jones BE. Sleep-wake related discharge properties of basal forebrain neurons recorded with micropipettes in head-fixed rats. J Neurophysiol 2004;92:1182–1198. [PubMed: 15028746]

Lee MG, Hassani O, Jones BE. Discharge of identified orexin/hypocretin neurons across the sleep-waking cycle. J Neurosci 2005a;25:6716–6720. [PubMed: 16014733]

Lee MG, Hassani OK, Alonso A, Jones BE. Cholinergic basal fore-brain neurons burst with theta during waking and paradoxical sleep. J Neurosci 2005b;25:4365–4369. [PubMed: 15858062]

Li Y, Gao XB, Sakurai T, van den Pol AN. Hypocretin/orexin excites hypocretin neurons via a local glutamate neuron—a potential mechanism for orchestrating the hypothalamic arousal system. Neuron 2002;36:1169–1181. [PubMed: 12495630]

Lin L, Faraco J, Li R, Kadotani H, Rogers W, Lin X, Qiu X, de Jong PJ, Nishino S, Mignot E. The sleep disorder canine narcolepsy is caused by a mutation in the hypocretin (orexin) receptor 2 gene. Cell 1999;98:365–376. [PubMed: 10458611]

Manns ID, Alonso A, Jones BE. Discharge profiles of juxtacellularly labeled and immunohistochemically identified GABAergic basal fore-brain neurons recorded in association with the electroencephalogram in anesthetized rats. J Neurosci 2000;20:9252–9263. [PubMed: 11125003]

Mileykovskiy BY, Kiyashchenko LI, Siegel JM. Behavioral correlates of activity in identified hypocretin/orexin neurons. Neuron 2005;46:787–798. [PubMed: 15924864]

Millhouse OE. A Golgi study of the descending medial forebrain bundle. Brain Res 1969;15:341–363. [PubMed: 4899094]

Modirrousta M, Mainville L, Jones BE. GABAergic neurons with alpha2-adrenergic receptors in basal forebrain and preoptic area express c-Fos during sleep. Neuroscience 2004;129:803–810. [PubMed: 15541901]

Modirrousta M, Mainville L, Jones BE. Orexin and MCH neurons express c-Fos differently after sleep deprivation vs. recovery and bear different adrenergic receptors. Eur J Neurosci 2005;21:2807–2816. [PubMed: 15926928]

Nishino S, Tafti M, Reid MS, Shelton J, Siegel JM, Dement WC, Mignot E. Muscle atonia is triggered by cholinergic stimulation of the basal forebrain: implication for the pathophysiology of canine narcolepsy. J Neurosci 1995;15:4806–4814. [PubMed: 7623112]

Paxinos, G.; Watson, C. The rat brain in stereotaxic coordinates. Sydney: Academic Press; 1986.

Peyron C, Tighe DK, van den Pol AN, de Lecea L, Heller HC, Sutcliffe JG, Kilduff TS. Neurons containing hypocretin (orexin) project to multiple neuronal systems. J Neurosci 1998;18:9996–10015. [PubMed: 9822755]

Peyron C, Faraco J, Rogers W, Ripley B, Overeem S, Charnay Y, Nevsimalova S, Aldrich M, Reynolds D, Albin R, Li R, Hungs M, Pedrazzoli M, Padigaru M, Kucherlapati M, Fan J, Maki R, Lammers GJ, Bouras C, Kucherlapati R, Nishino S, Mignot E. A mutation in a case of early onset narcolepsy and a generalized absence of hypocretin peptides in human narcoleptic brains. Nat Med 2000;6:991–997. [PubMed: 10973318]

Pfeiffer F, Simler R, Grenningloh G, Betz H. Monoclonal antibodies and peptide mapping reveal structural similarities between the subunits of the glycine receptor of rat spinal cord. Proc Natl Acad Sci U S A 1984;81:7224–7227. [PubMed: 6095276]

Sakurai T. Roles of orexin/hypocretin in regulation of sleep/wakefulness and energy homeostasis. Sleep Med Rev 2005;9:231–241. [PubMed: 15961331]

Sakurai T, Nagata R, Yamanaka A, Kawamura H, Tsujino N, Muraki Y, Kageyama H, Kunita S, Takahashi S, Goto K, Koyama Y, Shioda S, Yanagisawa M. Input of orexin/hypocretin neurons revealed by a genetically encoded tracer in mice. Neuron 2005;46:297–308. [PubMed: 15848807]

Saper CB, Chou TC, Scammell TE. The sleep switch: hypothalamic control of sleep and wakefulness. Trends Neurosci 2001;24:726–731. [PubMed: 11718878]

Sassoe-Pognetto M, Fritschy JM. Mini-review: gephyrin, a major postsynaptic protein of GABAergic synapses. Eur J Neurosci 2000;12:2205–2210. [PubMed: 10947798]

Sassoe-Pognetto M, Kirsch J, Grunert U, Greferath U, Fritschy JM, Mohler H, Betz H, Wassle H. Colocalization of gephyrin and GABAA-receptor subunits in the rat retina. J Comp Neurol 1995;357:1–14. [PubMed: 7673460]

Sassoe-Pognetto M, Panzanelli P, Sieghart W, Fritschy JM. Colocalization of multiple GABA(A) receptor subtypes with gephyrin at postsynaptic sites. J Comp Neurol 2000;420:481–498. [PubMed: 10805922]

Sassoe-Pognetto M, Utvik JK, Camoletto P, Watanabe M, Stephenson FA, Bredt DS, Ottersen OP. Organization of postsynaptic density proteins and glutamate receptors in axodendritic and

dendrodendritic synapses of the rat olfactory bulb. J Comp Neurol 2003;463:237–248. [PubMed: 12820158]

Semba K, Reiner PB, McGeer EG, Fibiger HC. Brainstem projecting neurons in the rat basal forebrain: neurochemical, topographical, and physiological distinctions from cortically projecting cholinergic neurons. Brain Res Bull 1989;22:501–509. [PubMed: 2469525]

Sheng M, Pak DT. Ligand-gated ion channel interactions with cytoskeletal and signaling proteins. Annu Rev Physiol 2000;62:755–778. [PubMed: 10845110]

Siegel JM. Hypocretin (orexin): role in normal behavior and neuropathology. Annu Rev Psychol 2004;55:125–148. [PubMed: 14744212]

Swanson LW. An autoradiographic study of the efferent connections of the preoptic region in the rat. J Comp Neurol 1976;167:227–256. [PubMed: 819466]

Swanson LW, Sanchez-Watts G, Watts AG. Comparison of melanin-concentrating hormone and hypocretin/orexin mRNA expression patterns in a new parceling scheme of the lateral hypothalamic zone. Neurosci Lett 2005;387:80–84. [PubMed: 16084021]

Szymusiak R, McGinty D. Sleep suppression following kainic acid-induced lesions of the basal forebrain. Exp Neurol 1986a;94:598–614. [PubMed: 3780909]

Szymusiak R, McGinty D. Sleep-related neuronal discharge in the basal forebrain of cats. Brain Res 1986b;370:82–92. [PubMed: 3708324]

Szymusiak R, Alam N, McGinty D. Discharge patterns of neurons in cholinergic regions of the basal forebrain during waking and sleep. Behav Brain Res 2000;115:171–182. [PubMed: 11000419]

Taheri S, Zeitzer JM, Mignot E. The role of hypocretins (orexins) in sleep regulation and narcolepsy. Annu Rev Neurosci 2002;25:283–313. [PubMed: 12052911]

Takamori S, Riedel D, Jahn R. Immunoisolation of GABA-specific synaptic vesicles defines a functionally distinct subset of synaptic vesicles. J Neurosci 2000;20:4904–4911. [PubMed: 10864948]

Thannickal TC, Moore RY, Nienhuis R, Ramanathan L, Gulyani S, Aldrich M, Cornford M, Siegel JM. Reduced number of hypocretin neurons in human narcolepsy. Neuron 2000;27:469–474. [PubMed: 11055430]

van den Pol AN. Hypothalamic hypocretin (orexin): robust innervation of the spinal cord. J Neurosci 1999;19:3171–3182. [PubMed: 10191330]

Vazquez J, Baghdoyan HA. Basal forebrain acetylcholine release during REM sleep is significantly greater than during waking. Am J Physiol Regul Integr Comp Physiol 2001;280:R598–601. [PubMed: 11208592]

Veening JG, Swanson LW, Cowan WM, Nieuwenhuys R, Geeraedts LMG. The medial forebrain bundle of the rat. II. An autoradiographic study of the topography of the major descending and ascending components. J Comp Neurol 1982;206:82–108. [PubMed: 6980232]

Wouterlood FG, van Haeften T, Blijleven N, Perez-Templado P, Perez-Templado H. Double-label confocal laser-scanning microscopy, image restoration, and real-time three-dimensional reconstruction to study axons in the central nervous system and their contacts with target neurons. Appl Immunohistochem Mol Morphol 2002;10:85–95. [PubMed: 11893043]

Wouterlood FG, Bockers T, Witter MP. Synaptic contacts between identified neurons visualized in the confocal laser scanning microscope. Neuroanatomical tracing combined with immunofluorescence detection of post-synaptic density proteins and target neuron-markers. J Neurosci Methods 2003;128:129–142. [PubMed: 12948556]

Wu M, Shanabrough M, Leranth C, Alreja M. Cholinergic excitation of septohippocampal GABA but not cholinergic neurons: implications for learning and memory. J Neurosci 2000;20:3900–3908. [PubMed: 10804229]

Yamanaka A, Beuckmann CT, Willie JT, Hara J, Tsujino N, Mieda M, Tominaga M, Yagami K, Sugiyama F, Goto K, Yanagisawa M, Sakurai T. Hypothalamic orexin neurons regulate arousal according to energy balance in mice. Neuron 2003a;38:701–713. [PubMed: 12797956]

Yamanaka A, Muraki Y, Tsujino N, Goto K, Sakurai T. Regulation of orexin neurons by the monoaminergic and cholinergic systems. Biochem Biophys Res Commun 2003b;303:120–129. [PubMed: 12646175]

Yoshida K, McCormack S, Espana RA, Crocker A, Scammell TE. Afferents to the orexin neurons of the rat brain. J Comp Neurol 2006;494:845–861. [PubMed: 16374809]

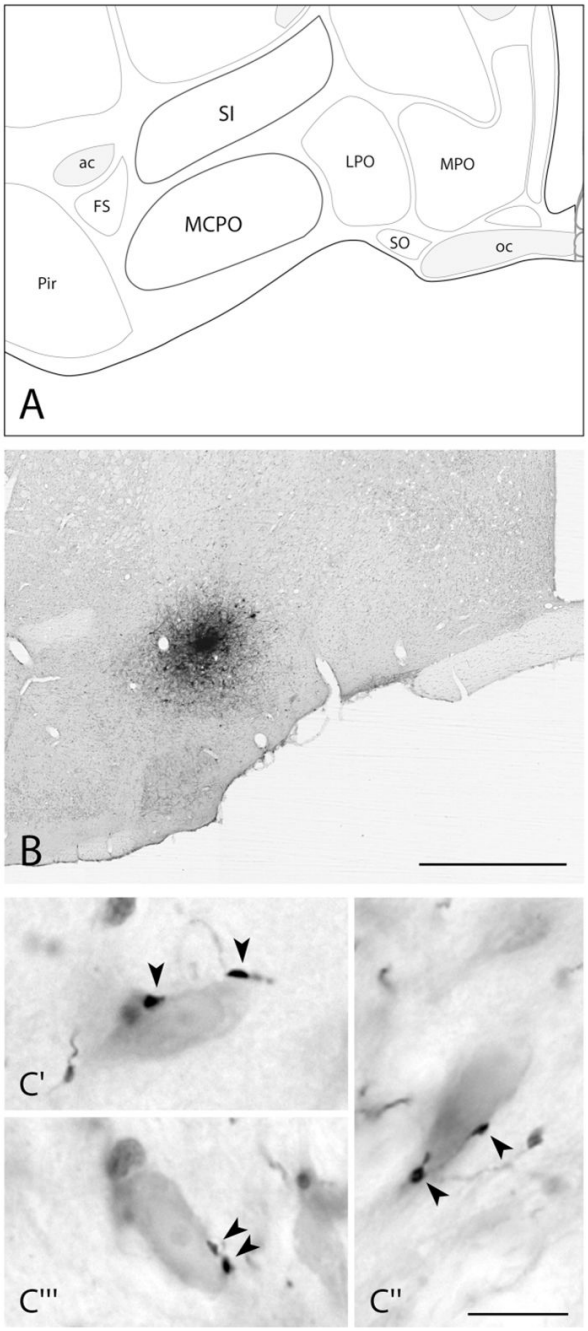

Fig. 1.

BDA injection site in BF and anterogradely labeled BF terminals in the LH. **A:** Atlas section through the cholinergic cell area (MCPO-SI) where iontophoretic applications of BDA were placed. **B:** Composite image of typical BDA injection site (processed using ABC with DAB-Ni and counterstained for Nissl with neutral red). Note the small size and restricted location of BDA injection site in the MCPO. **C:** High-magnification images showing BDA+ axonal varicosities (arrowheads) contacting Nissl-stained cell bodies located in dorsal (C′), middle (C ″), and ventral (C‴) portions of the LH area. Scale bars = 1 mm in B; 10 μm in all C.

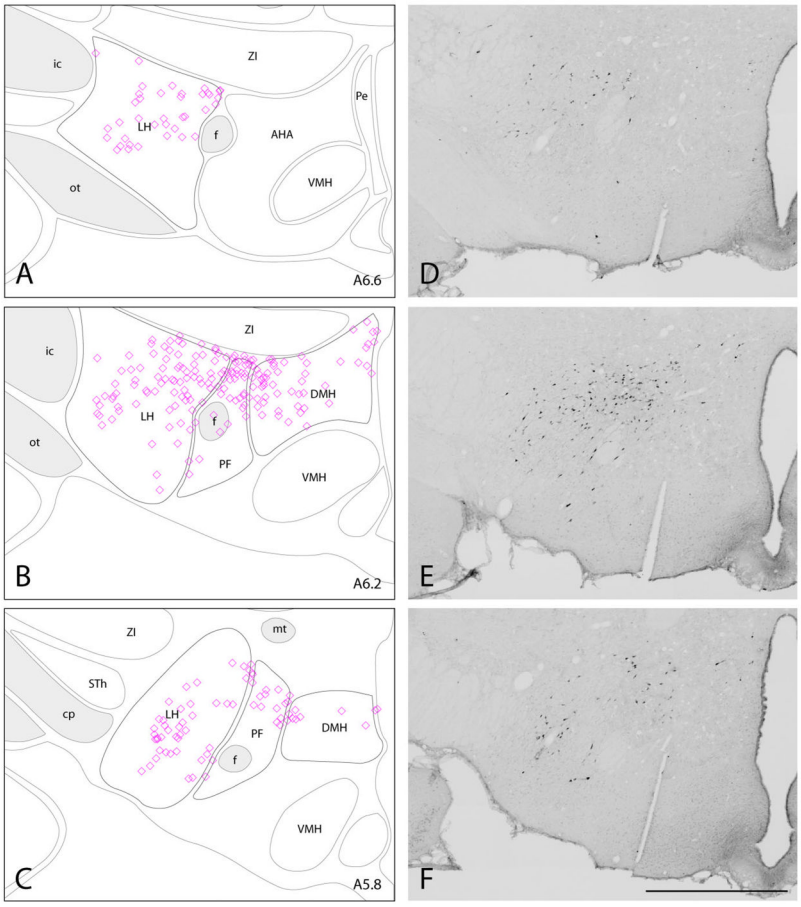

Fig. 2.

Distribution of Orx+ neurons at three levels through the tuberal hypothalamus. **A–C:** Mapping of Orx+ neurons within contours of the LH, PF, and DMH at A6.6 (A), A6.2 (B), and A5.8 (C) levels, based on the material presented in D–F, respectively. Some few scattered Orx+ neurons within contours of the AHA, Pe and ZI are not shown in the mapping. **D–F:** Composite images of sections immunostained for Orx-A (with DAB) showing the distribution of Orx+ neurons in the hypothalamus at A6.6 (D), A6.2 (E), and A5.8 (F). Scale bar = 1 mm in F (applies to D–F).

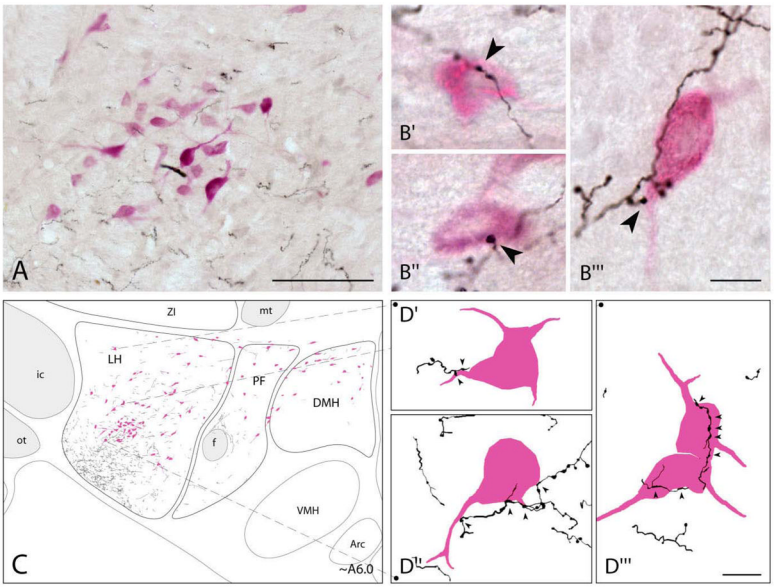

Fig. 3.

Distribution of BDA-labeled fibers in relation to Orx+ neurons. **A:** Low-magnification composite image of BDA+ axons (in black, DAB-Ni) and Orx+ cells (in fuchsia, ANPB) in the LH at ~A6.0. **B:** High-magnification images showing BDA+ varicosities (arrowheads) in contact with Orx+ neurons in the LH (B′, B″, and B‴). **C:** Tracing and mapping of all BDA+ fibers and Orx+ neurons in the tuberal hypothalamus at ~A6.0 μm (from IA0). From coarse fibers within the ventrolateral MFB, fine varicose collaterals extended dorsally and medially to reach Orx+ cells through the LH. Some fibers also extended medially into the PF and DMH. **D:** High magnification of elements depicted in C, showing contacts of BDA+ axons by varicosities on proximal dendrites or soma of Orx+ cells located in the dorsal (D′) or central (D″ and D‴) region of the LH. Tonal range for each RGB channel as well as brightness and contrast adjustment were made for pictures in A and B. Scale bars = 100 μm in A; 10 μm in B,D.

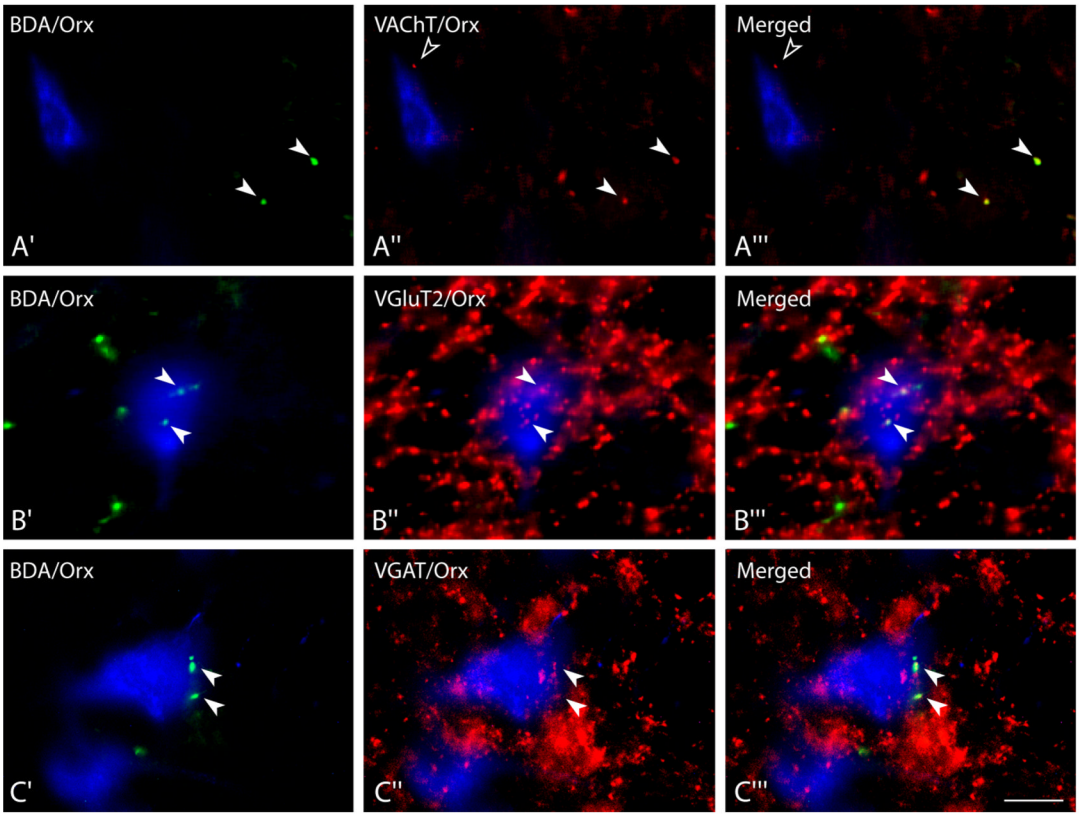

Fig. 4.

VAChT+, VGluT2+ or VGAT+, BDA-labeled varicosities in relation to Orx+ neurons viewed by epifluorescent microscopy. In each case, BDA is green (Cy2), VTP red (Cy3), and Orx blue (AMCA in A or Cy5 in B and C). **A:** BDA+ [VAChT+] terminals in the vicinity of an Orx+ neuron. BDA+ terminals (solid arrowheads in A′) located in the vicinity, yet not close to an Orx+ neuron (left), are positive for the VAChT protein (solid arrowheads in A″), as evident in the merged image (in yellow, solid arrowheads in A‴). A VAChT+ terminal that is not BDA + (open arrowhead) is closer to the Orx+ cell body. Note also the sparse number of VAChT+ varicosities in the vicinity of Orx+ neurons. **B:** BDA+ [VGluT2+] terminals in close proximity to Orx+ neurons. Two small BDA+ terminals (solid arrowheads in B′) over an Orx+ cell body are positive for the VGluT2 protein (solid arrowheads in B″), as evident in the merged image (in yellow, solid arrowheads in B‴). Note also the relatively large number of VGluT2+ varicosities in close proximity to the Orx+ neurons. **C:** BDA+ [VGAT+] terminals over Orx+ neurons. Two BDA+ terminals (solid arrowheads in C′) in close proximity to an Orx+ neuron are positive for VGAT (solid arrowheads in C″), as evident in the merged image (in yellow, solid arrowheads in C‴). In all images, tonal range was adjusted for each RGB channel individually. Scale bar = 10 μm in C‴ (applies to A–C).

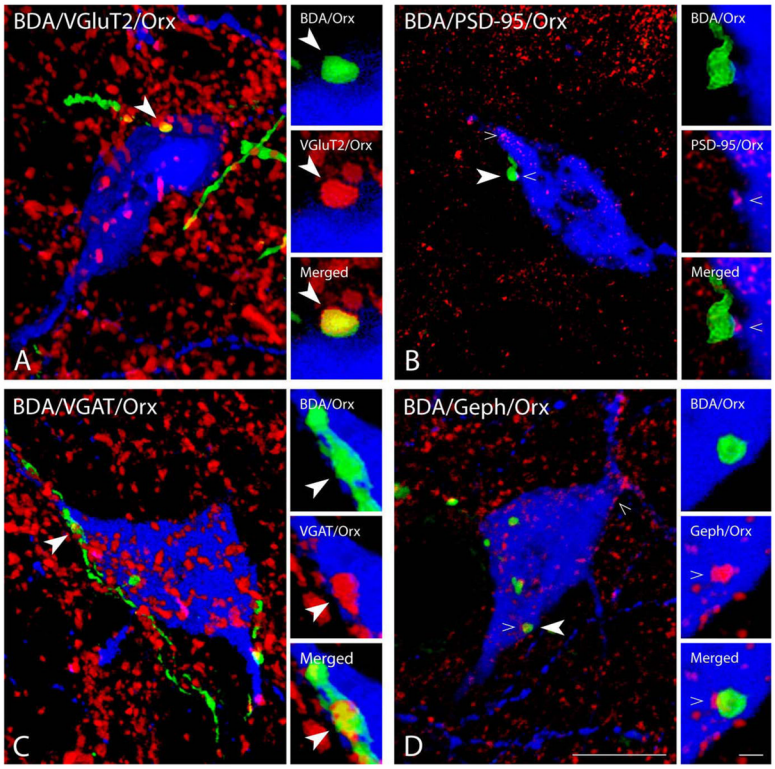

Fig. 5.

The presence of presynaptic VGluT2 or VGAT and postsynaptic PSD-95 or Gephyrin (Geph) proteins in contacts between BDA-labeled varicosities and Orx+ neurons. **A:** Rendered 3D confocal image (16 serial 0.50-μm thick optical sections) of a BDA-labeled axon (in green, Cy2), whose varicosities (in yellow) are positive for VGluT2 (in red, Cy3). One of these varicosities is in apposition (arrowhead) to an Orx+ neuron (in pseudocolor blue, Cy5), as evident in the rendered zoom images on the right (6 serial 0.5-μm thick optical sections) depicting in detail the relation between the BDA+ varicosity (top) or the contained VGluT2 (middle) with the Orx+ neuron surface and showing the three elements together in the merged image (bottom). Note also on the left other VGluT2+ varicosities in contact with the Orx+ neuron. **B:** Rendered 3D confocal image (9 serial 0.33-μm thick optical sections) of a BDA+ varicosity (arrowhead, in green, Cy2) facing a PSD-95+ profile (opposite pointer, in pseudocolor red, Cy5) located between the varicosity and the surface of the Orx+ neuron (in pseudocolor blue, Cy3). As evident in the zoom rendered images on the right (13 serial 0.33-μm thick optical sections), the BDA+ varicosity is apposed to the Orx+ process (top image), opposite the PSD-95+ punctum, which is on the surface of the Orx+ process (pointer, middle image) and between the BDA+ varicosity and the Orx+ process (pointer in the merged image, bottom). Note the presence of other PSD-95+ puncta over the Orx+ neuron (upper pointer) at the left panel. **C:** Rendered 3D confocal image (28 serial 0.5-μm thick optical sections) of a BDA-labeled axon (in green, Cy2), from which most varicosities (in yellow) are positive for VGAT (in red, Cy3) and come into contact (large arrowhead) with the dendrites and soma of the Orx+ neuron. As seen in the rendered zoom images on the right (8 serial 0.5-μm thick optical sections), the BDA+ varicosity (top image) containing VGAT (middle image) appears to be in contact with the surface of the Orx+ neuron (merged image, bottom). Note in the left image other VGAT+ varicosities also appear to appose the Orx+ neuron. **D:** Rendered 3D confocal image (14 serial 0.33-μm thick optical sections) of BDA-labeled axonal varicosities (arrowhead, green, Cy2) facing Geph+ puncta (facing pointer, pseudocolor red, Cy5) over an Orx+ neuron (pseudocolor blue, Cy3). As evident in the zoom rendered images at the right (12

serial 0.33-+m thick optical sections), the apposition of the BDA+ varicosity with the Orx+ neuron (top image) is associated with a Geph+ punctum on the surface of the Orx+ neuron (pointer, middle image) and between the BDA+ varicosity and the Orx+ neuron (merged image, pointer, bottom). Note the presence of other Geph+ puncta over the Orx+ neuron (upper pointers) in the left panel. Deconvolution iterative restoration (see Materials and Methods) was applied to the Cy5 channel (in B and C, left panels, and in A–D, right panels), the Cy3 channel (in C, left panel, and in C,D, right panels) and the Cy2 channel (in B–D). Tonal range adjustments for each individual RGB channel were made for all pictures. Scale bars = 10 μm in left large panel in D (applies to large left panels in A–C); 1 μm in D, zoom bottom image (applies to zoom images in A–C).

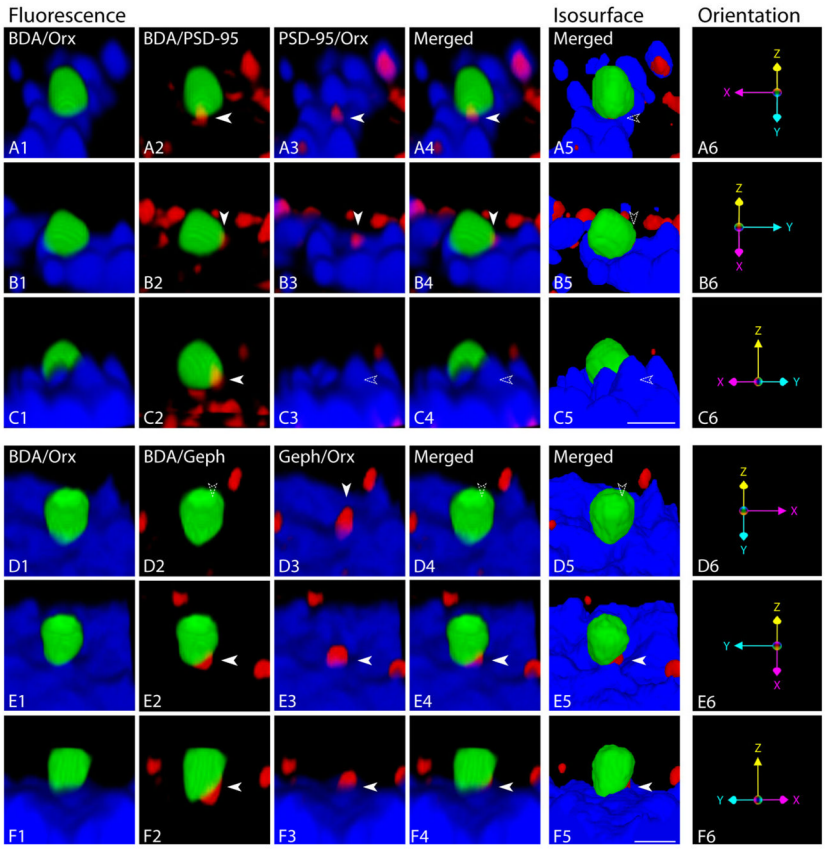

Fig. 6.

3D localization of postsynaptic proteins PSD-95 or gephyrin (Geph) between BDA+ terminals and Orx+ neurons. **A–C:** Orthogonal views (see below) of a high-resolution rendered confocal 3D image (40 serial ~0.06-μm thick optical sections) in semitransparent fluorescence rendering (columns 1–4) or opaque isosurface (column 5) views of a single contact between a BDA+ varicosity (in green, Cy2) and an Orx+ proximal dendrite (in blue, Cy3), with the presence of PSD-95+ puncta (in red, Cy5) between the varicosity and dendrite. The BDA+ varicosity is in contact with the Orx+ process (A1–C1), and in clear apposition to a PSD-95+ profile (solid arrowheads in A2–C2,), which is in turn located on the surface of the Orx+ neuron (solid arrowheads in A3,B3). The localization of the PSD-95+ profile between the two structures is evident in the triple merged fluorescent image (solid arrowheads in A4,B4) as well as in the triple merged isosurface rendering image, where the punctum appears almost completely occluded (dotted arrowheads in A5–C5). The PSD-95+ punctum is completely occluded in certain of the orthogonal views (dotted arrowheads in C3–C5). A6–C6: Representation of the three orthogonal views with orientation markers showing the X, Y, Z axes. **D–F:** Orthogonal views of a high-resolution rendered confocal 3D image (38 serial ~0.08-μm thick optical sections) in semitransparent fluorescence rendering (columns 1–4) or opaque isosurface rendering (column 5) views of a single contact between a BDA+ varicosity (in green, Cy2) and an Orx+ soma (in blue, Cy3), with the presence of Geph+ puncta (in red, Cy5) between the terminal and soma. The BDA+ varicosity is in contact with an Orx+ soma (D1–F1) and in clear apposition to a Geph+ profile (solid arrowheads in E2,F2), which is in turn located on the surface of the Orx+ neuron (solid arrowheads in D3–F3). The localization of the Geph+ profile between the two structures is evident in the triple merged fluorescent image (solid arrowheads in E4,F4) as well as in the triple merged isosurface image (solid arrowheads in E5,F5). Note the relative occlusion of the Geph+ profile in the rendered isosurface images,

evidencing its location between the two structures. Due to the orthogonal views, the Geph+ puncta are completely occluded in some of them (dotted arrowheads in D2,D4,D5). D6–F6: Representation of the three orthogonal views with orientation markers showing the X, Y, Z axes. Deconvolution iterative restoration (see Materials and Methods) was applied to the Cy5, Cy3, and Cy2 channels. Scale bars = 1 μm in C5 (applies to A–C), and in F5 (applies to D–F).

TABLE 1

Primary Antibodies (AB) for Immunostaining of Orexin (Orx), Vesicular Transporter Proteins (VTPs) or Postsynaptic Proteins (PSPs)

Antigen	Host sp	Source	Cat. #	Immunogen	Specificity
Orx					
Orx-A	Rb	Phoenix[1]	H-003-30	Full 33 AA Orx-A peptide sequence from rat (EPLPDCCRQKTCSCRLYELLHGAGNHAAGILTL)[2]	By WB the AB recognizes a ≈3.5 kD band from rat brain, corresponding to the Orx-A peptide[2]
Orx-A	Gt	Santa Cruz[3]	sc-8070	Peptide mapping at the C-terminus of human Orx-A (AA 48–66 of the Orx precursor, identical to corresponding mouse sequence)[4]	AB reacts with Orx-A of mouse, rat and human by WB, immunostaining blocked with antigen peptide (sc-8070 P) and pattern of staining identical to that with Orx-A (Rb) H-003-30 (Phoenix)[5]
VTPs					
VAChT	Gt	Chemicon[6]	AB1578	Peptide corresponding to C-terminus of cloned rat VAChT[7] (CSPPGPFDGCEDDYNYYSRS)[8]	By WB the AB recognizes a ≈65–70 kD band corresponding to VAChT protein[7]
VAChT	Rb	Sigma[9]	V5387	Peptide corresponding to AA 512–530 of C-terminus of cloned rat VAChT (K-SPPGPFDGCEDDYNYYSRS)[10]	By WB the AB recognizes a ≈67–70 kD band, corresponding to VAChT protein[10]
VGluT2	Rb	Gift RHE[11]	-	GST fusion protein containing AA 519–582 of rat DNPi (VGluT2)[12]	By WB the AB recognizes a ≈50–62 kD band from rat brain[12]
VGAT	Rb	Chemicon	AB5062P	Peptide corresponding to 17 AA near C-terminus region of rat VGAT (VHSLEGLIEAYRTNAED)[13]	By WB the AB recognizes a band at ≈55–60 kD[13]
PSPs					
PSD-95	Ms	ABR[14]	MA1-045	Purified recombinant of rat PSD-95[15]	By WB the AB recognizes a ≈95 kDa protein and a slightly larger species from rat brain extracts[15]
Geph	Ms	Sy-Sy[16]	147011	Purified rat gephyrin[17]	By WB the AB recognizes a ≈93 kD band. It detects a N-terminus epitope[18]

AA, amino acid; AB, antibody; DNPi, differentiation-associated Na^+-dependent phosphate transporter; Geph, gephyrin; Gt, goat; Ms, mouse (monoclonal); Rb, rabbit; sp, species; WB, western blot.

[1] Phoenix Pharmaceuticals, Belmont, CA.

[2] http://www.phoenixpeptide.com/Catalog%20Files/Orexins%20Section/OrexinsHypocretinspage.htm

[3] Santa Cruz Biotechnology, Santa Cruz, CA.

[4] Information provided by Santa Cruz data sheet and technical service.

[5] Information on WB provided by Santa Cruz data sheet and technical service, blocking experiments carried out in our lab with the Santa Cruz antigen peptide and immunostaining of Orx cell population compared for two antibodies in our lab in this and previous studies (Modirrousta et al., 2005).

[6] Chemicon International, Temecula, CA.

[7] http://www.chemicon.com/Product/ProductDataSheet.asp?ProductItem=AB1578

[8] Supplied by Chemicon on request.

[9] Sigma, St. Louis, MO.

[10] http://www.sigmaaldrich.com/sigma/datasheet/v5387dat.pdf

[11] Gift from R.H. Edwards and R.T. Fremeau Jr.

[12] Fremeau et al., 2001.

[13] http://www.chemicon.com/Product/ProductDataSheet.asp?ProductItem=AB5062P

[14] ABR: Affinity BioReagents, Golden, CO.

[15] http://www.bioreagents.com/index.cfm/fuseaction/products.print/Product/MA1-045

[16] SY-SY: Synaptic Systems, Goettingen, Germany.

[17] http://www.sysy.com/gephyrin/gephy_fs.html

[18] Pfeiffer et al., 1984.

TABLE 2

Combination and Sequential Processing of Primary and Secondary Antibodies along with Streptavidin (SA) Used for Triple Fluorescent Staining of Orexin (Orx), Vesicular Transporter Proteins (VTPs), or Postsynaptic Proteins (PSPs) and Biotinylated Dextran Amine (BDA)

	1ry AB (overnight)[1]			2ry AB (3 hours)		SA (3 hours)		
Series	**Antigen**	**Hostsp**	**Dilution**	**IgG (Dky)[2,3]**	**Dilution**	**SA**	**Dilution**	**n[4]**
BDA/VTP/Orx								
BDA/VAChT/Orx	VAChT	Gt	1:1000	Anti-Gt-Cy3	1:800	SA-Cy2	1:800	4
	Orx-A	Rb	1:200	Anti-Rb-AMCA	1:100			
BDA/VAChT/Orx	VAChT	Gt	1:1000	Anti-Gt-Cy3	1:800	"	"	2
	Orx-A	Rb	1:200	Anti-Rb-Cy5	1:800			
BDA/VAChT/Orx	VAChT	Rb	1:5000	Anti-Rb-Cy3	1:800	"	"	5
	Orx-A	Gt	1:200	Anti-Gt-Cy5	1:800			
BDA/VGluT2/Orx	VGluT	Rb	1:5000	Anti-Rb-Cy3	1:800	"	"	4
	2Orx-A	Gt	1:200	Anti-Gt-AMCA	1:100			
BDA/VGluT2/Orx	VGluT	Rb	1:5000	Anti-Rb-Cy3	1:800	"	"	11
	2Orx-A	Gt	1:200	Anti-Gt-Cy5	1:800			
BDA/VGA T/Orx	VGA T	Rb	1:250	Anti-Rb-Cy3	1:800	"	"	4
	Orx-A	Gt	1:200	Anti-Gt-AMCA	1:100			
BDA/VGA T/Orx								
BDA/PSP/Orx	VGA T	Rb	1:250	Anti-Rb-Cy3	1:800	"	"	11
	Orx-A	Gt	1:200	Anti-Gt-Cy5	1:800			
BDA/PSD-95/Orx	PSD-95	Ms	1:100	Anti-Ms-Cy5	1:800	SA-Cy2	1:800	3
	Orx-A	Gt	1:200	Anti-Gt-Cy3	1:800			
BDA/Geph/Orx	Geph	Ms	1:100	Anti-Ms-Cy5	1:800	"	"	3
	Orx-A	Gt	1:200	Anti-Gt-Cy3	1:800			

AB, antibody; AMCA, aminomethylcoumarin acetate; Cy2, cyanine; Cy3, indocarbocyanine; Cy5, indodicarbocyanine; Dky, donkey; Geph, gephyrin; Gt, goat; Ms, mouse (monoclonal); Rb, rabbit; sp, species.

[1] For sources and specificity of primary antibodies from different species, refer to Table 1.

[2] Jackson ImmunoResearch Laboratories, West Grove, PA.

[3] For multiple labeling (ML) with minimal crossreactivity (min X) to other species.

[4] n: number of cases (each case referring to an injection site and series from the same side of the brain, thus 1 or 2 per brain from 9 rats for a total of 16 injection sites selected for their placement in the MCPO/SI).

TABLE 3

Numbers and Proportions of Orx Cells and Orx+ Cells Contacted by BDA+ Varicosities Estimated across Hypothalamic Regions[1]

Hypothalamic region	LH	PF	DMH	Total
Single-immunostained Orx series[2]				
N° Orx cells	1770.7 ± 182.3	469.3 ± 21.3	917.3 ± 149.3	3157.3 ± 259.5
% Orx cells of Total across regions	**56.0** ± **3.0 %**	**15.2 3 2.0 %**	**28.8** ± **2.9 %**	**100 3 0.0 %**
Dual-immunostained BDA/Orx series[3]				
N° Orx+ cells	1216.0 ± 97.8	320.0 ± 37.0	576.0 ± 97.8	2122.0 ± 97.8
N° Orx+ cells contacted by a BDA + var. (Orx+:BDA+)	512.0 ± 110.9	42.7 ± 42.7	42.7 ± 21.3	597.3 ± 166.6
% Orx+ cells contacted by a BDA+ var. in each region	**41.4** ± **7.1 %**	**11.1** ± **11.1 %**	**8.9** ± **4.8 %**	**27.7** ± **6.6 %**

Data are presented as means ± SEM. DMH, dorsomedial hypothalamic nucleus; LH, lateral hypothalamus; PF, perifornical area; var., varicosity.

[1] Estimated numbers of cells and BDA-contacted cells were obtained by random systematic sampling of the hypothalamus at levels A6.6, A6.2 and A5.8 for LH, and levels A6.2 and A5.8 for PF and DMH using StereoInvestigator.

[2] Series from 3 different brains processed for single-immunostaining of Orx cells with DAB (see Methods).

[3] Series from 3 individual cases (injection sites) processed for dual-immunostaining of BDA (with DAB-Ni) and Orx (with ANPB, see Materials and Methods).

TABLE 4

Numbers and Proportions of Orx+ Cells Contacted by BDA+ Varicosities Positive for Vesicular Transporter Proteins (VTP+), and Numbers and Proportions of BDA+ [VTP+] Varicosities in Contact with Orx+ Cells in the Lateral Hypothalamus (LH)[1]

Triple-immunostained BDA/VTP/Orx series	VAChT	VGluT2	VGAT
N° Orx+ cells contacted by BDA+ var. (Orx+:BDA+) in each series	548.3 ± 68.3	532.7 ± 109.7	595.3 ± 109.7
N° Orx+ cells contacted by BDA+ [VTP+] var. (Orx+:BDA+ [VTP+])[2]	15.7 ± 15.7	188.0 ± 81.4	376.0 ± 27.1
% Orx+ cells contacted by BDA+ [VTP+] var.[2]	**3.7 ± 3.7 %**	**31.4 ± 9.4 %**	**66.7 ± 11.2 %**
N° BDA+ var. in contact with Orx+ cells (BDA+: Orx+) in each series	908.6 ± 122.4	1096.7 ± 180.7	1457.0 ± 204.9
N° BDA+ [VTP+] var. in contact with an Orx+ cells (BDA+ [VTP+]:Orx+)[2]	15.7 ± 15.7	203.7 ± 95.3	814.7 ± 87.2
% BDA+ [VTP+] var. in contact with Orx+ cells[2]	**2.2 ± 2.2 %**	**16.6 ± 6.2 %**	**57.8 ± 8.7 %**

Data are presented as means ± SEM. var., varicosity.

[1] Estimated numbers of cells were obtained by random systematic sampling of the LH area at levels A6.6, A6.2 and A5.8 using StereoInvestigator from three individual cases (injection sites).

[2] According to a non-parametric Kruskal-Wallis test, the different VTP+ varicosities differed significantly according to the numbers ($H = 6.587$, $P = 0.037$) and proportions ($H = 7.261$, $P = 0.027$) of Orx+ neurons contacted by BDA+ [VTP+] and to the numbers ($H = 6.587$, $P = 0.037$) and proportions ($H = 6.938$, $P = 0.031$) of BDA+ [VTP+] varicosities contacting Orx+ neurons.